

## ELECTRON YIELDS FROM SPACECRAFT MATERIALS\*

K. Yang, W. L. Gordon, and R. W. Hoffman  
Case Western Reserve University  
Cleveland, Ohio 44106

Photoyields and secondary electron emission (SEE) characteristics have been determined under UHV conditions for a group of insulating materials used in spacecraft applications. The SEE studies were carried out with a pulsed primary beam while photoyields were obtained with a chopped photon beam from a Kr resonance source with major emission at 123.6 nm. This provides a photon flux close to that of the Lyman  $\alpha$  in the space environment. Yields per incident photon are obtained relative to those from a freshly evaporated and air oxidized Al surface. Samson's value of  $\sim 2.4\%$  is taken for the Al yield. Results are presented for Kapton, FEP Teflon, the borosilicate glass covering of a shuttle tile, and spacesuit outer fabric.

## INTRODUCTION

In the use of NASCAP (ref. 1), a computer code which simulates charging of a three-dimensional object in space, it is important to have data on electron yields from the various materials comprising the spacecraft surface. In an on-going program (ref. 2) pulsed primary electron beam methods have been developed to avoid charging effects in yield measurements from insulating surfaces. These studies are carried out in an ultra high vacuum system employing a commercial double pass CMA which permits sequential Auger analysis of the surface and target current measurements of electron yield data as a function of the primary energy, EP. This pulsed beam technique has been extended to permit vacuum ultraviolet (VUV) photoyield measurements of these insulating surfaces: Kapton, Teflon, the borosilicate glass surface of shuttle tile, and the outer fabric of spacesuit material.

## EXPERIMENTAL TECHNIQUES

Target current measurements of secondary yield by pulsed electron beam methods, introduced in a study of insulating materials, have already been discussed in reference 2. We describe here the adaptation of this approach to obtain photoyields. The spectral range of interest is restricted to the VUV because of the photoemission threshold of most materials. We have chosen to carry out these preliminary experiments with an Opthos VUV krypton source powered by a Kiva Model MPG 4 microwave generator producing resonance lines at 116.6 and 123.6 nm with a relative intensity of approximately 1 to 7 respectively (or 1 to 15 after transmission through the  $MgF_2$  windows). This provides a reasonable approximation to the relevant portion of the solar spectrum with its intense Lyman  $H_\alpha$  line.

\*Work performed under NASA Grant No. NSG-3197

As illustrated in figure 1, the Kr source is mounted on the end of a cylindrical housing containing a camera shutter to permit chopping of the light beam. The beam travels in an argon atmosphere to avoid air absorption and enters the UHV system through a MgF<sub>2</sub> window. The incident beam intensity is determined by irradiating a freshly evaporated and air oxidized Al film of ~ 150 nm thickness deposited on a glass substrate and using Samson's value (ref. 3) of 2.4% yield per incident photon at the Lyman H<sub>α</sub>. The yield from freshly evaporated samples is typically 50% greater than that from samples exposed to air for about 10 minutes, which corresponds to an essentially saturated value. It is this result which we assume corresponds to Samson's yield but have not placed this on an absolute basis as yet. Samples to be studied and the Al detector are mounted on the faces of the six-sided rotatable carousel.

A cylindrical cup collector electrode was mounted facing and surrounding the sample on the target as shown in figure 1. The collimated UV beam irradiates the sample by passing through an aperture on the axis of the collector. Our usual procedure was to measure collector current with the collector biased + 22.5 V relative to the grounded target. Typical currents ranged from 0.5 nA for relatively high yield materials down to 5 to 10 pA for the lowest yields. Although the shutter is capable of 1 millisecond pulse lengths, we have been able to avoid charging with pulses as long as 1 second. This has permitted use of a fast response chart recorder to obtain a plateau value for the collector current during each pulse.

## MATERIALS

Only insulating materials were studied in this investigation and all samples were obtained from NASA LeRC. Table I summarizes the materials studied and includes the preparation of rear surfaces since good electrical contact to the target is important. Approximately 2 cm x 2 cm samples were used in the photoyield studies with approximately 1 cm x 1 cm sizes employed in electron yield work. Dust particles were removed by blowing dry nitrogen across the surface but no other cleaning steps were used.

Square samples were cut from the ~ .5 mm thick borosilicate glass surface coating of the shuttle tile with a thin rotating disk. The silica fiber backing material was brushed away to permit good contact with indium foil in which the sample was embedded. An Al backing was evaporated on the rear surface of the outer fabric of the spacesuit later to provide better electrical contact with the target. As discussed later, this fabric and to a lesser extent the shuttle tile surface material, exhibited qualitatively stronger charging effects than did the Kapton and Teflon sheet. The greater average "thickness" of the cloth (~ 1 mm) means a reduced capacitance and thus an increased charging rate, per current pulse.

## RESULTS AND DISCUSSION

### Photoyields

Results, expressed as yields per incident photon, are summarized in table II with uncertainties based on the scatter of repeated measurements. Systematic uncertainties, such as the assumption that Samson's value of 2.4% yield applies to a

freshly evaporated and air oxidized Al surface or the effects of surface contamination, if present, are not included. Light pulses used in obtaining these results were generally 1 second in duration. A test for charge accumulation was done by repeated irradiation in the same location on the sample. Here we discovered that for the intensities employed, several (up to 10) pulses could be delivered to Kapton before the yield would begin to drop - such a drop is taken as our operational definition of charging. For the white shuttle tile, however, charging began after only one or two pulses and for the spacesuit fabric on the first pulse.

We experienced some difficulties in measuring the highly insulating materials having relatively low photoyields. This is due, in part, to low current values corresponding to the small yields such that the values are comparable to the noise. In the low yield insulating materials we also found a trend towards even lower values when we chose a modification of figure 1 consisting of grounding the collector, biasing the target - 22.5 V relative to ground and measuring the target current. This effect has not been explored in any detail as yet and may be spurious since it did not appear for the higher yield materials. We conclude that the results for both Teflon and the spacesuit fabric are preliminary and will require further study.

### Secondary Electron Yields

Results, using target current measurements with pulse beam methods as described in reference 2, were obtained for the materials in table I and are presented in figures 2 through 8 where only the total SEE coefficient,  $\sigma$ , is displayed. The primary electron beam was slightly defocused to  $\sim 2$  mm diameter and was moved to various locations on the sample during a series of measurements to reduce surface charging effects. Kapton and Teflon are displayed in figures 2 and 3 respectively. In figure 4, figures 2 and 3 are compared using a normalized scale on which  $\sigma/\sigma_{\max}$  is plotted vs.  $EP/EP_{\max}$  and it is clear that they are in close agreement. This is in contrast with the early work of Willis and Skinner (ref. 4) in which the Teflon data are well above the Kapton results on a similar normalized plot. Since very different samples were measured in these two investigations and different surface cleaning techniques were employed, we merely note these differences. Figures 5 and 6 present the SEE coefficients for the borosilicate glass shuttle tile surfaces in both as-received and sputtered condition. Some difficulties were experienced with charging of these samples because of their thickness ( $\sim 0.5$  mm) but we feel the results, while preliminary, are representative for reasons discussed later. Results from a sample of microscope cover glass are also included for comparison in figure 7. In each of these cases, sputtering sufficient to remove the nominal surface contamination has reduced the SEE coefficients substantially.

Figure 8 contains preliminary results for the outer fabric of the space suit. As noted earlier, the large sample thickness increased the tendency to charge. SEE results for all materials reported here are summarized in table III to provide a general comparison.  $EP_I$  and  $EP_{II}$  are the primary beam energies for which the total SEE coefficient is unity.

It is important to note that our usual method of obtaining SEE data for insulating materials appears to reduce charging problems. In biasing the target negatively then positively to obtain both the SEE coefficient,  $\sigma$  and  $\delta$ , at a given primary energy  $EP$ , the surface charge is reduced in the positive biased situation by electrons attracted back to the surface. This is illustrated by the record of multiple pulses (at  $EP = 500$  eV) delivered to the same location in the sample in figure 9. Here, the series of dots, although they show substantial scatter, tend to drop away much less

from the initial  $\sigma$  value than do the series of + points for which the target remained negatively biased. The latter points approach a unity value much more closely, indicating that charging has brought the surface potential close to the  $EP_{II}$ , the second cross-over value. The immediate effect of low energy electrons from a flood gun is also illustrated and appear somewhat more clearly in the highly charged case than in the alternating bias mode. One can conclude from these results that, though the data show substantial scatter, alternating the target bias helps to reduce surface charging effects.

### CONCLUSIONS

We have demonstrated reasonable results for both electron and photoyields from highly insulating materials where such data are not usually available. Pulsed irradiation methods were used to minimize charging effects.

### REFERENCES

1. Katz, K., Cassidy, J.J., Mandell, M.J., Schnuelle, R.W., Steen, P.G., and Roche, J.C.: The Capabilities of the NASA Charging Analyzer Program. Spacecraft Charging Technology - 1978, NASA Conf. Publ. 2071, 1979, p. 101.
2. Krainsky, I., Lundin, W., Gordon, W.L., and Hoffman, R.W.: Secondary Electron Emission Yield, Spacecraft Charging Technology - 1980. NASA Conf. Publ. 2182, 1981, p. 179.
3. Cairns, R.B. and Samson, J.A.R.: Metal Photocathodes as Secondary Standards for Absolute Intensity Measurements in the Vacuum Ultraviolet. J. Opt. Soc. Am. 56, 1966, p. 1568.
3. Willis, R.F. and Skinner, D.K.: Secondary Electron Emission Yield Behavior of Polymers. Sol. St. Comm. 13, 1973, p. 685.

TABLE I - MATERIALS STUDIES

Material	Back Surface
Thermal Blanket	
Kapton, 2 mil	Al
FEP Teflon 2 mil	Ag/Inconel
Shuttle Tile	
White borosilicate glass outer coating	In Foil*
Black borosilicate glass outer coating	In foil
Space Suit Components	
Outer fabric (ST11 G041-01)	Evaporated Al layer

\* Embedded in 0.5 mm In foil without covering sample surface.

TABLE II - PHOTOYIELDS

Material	Photoyield (%)
Kapton	0.65 ± 0.03
FEP Teflon	0.04 ± 0.03
White Shuttle Tile surface	0.2 ± 0.03
Black Shuttle Tile surface	0.3 ± 0.03
Outer fabric of space suit	0.06 ± 0.03

TABLE III - SUMMARY OF SEE RESULTS

Sample	$\sigma_{max}$	$EP_{max}$ (KeV)	$E_1$ (KeV)	$E_2$ (KeV)
Kapton	1.8	0.2	0.05	0.7
FEP Teflon	2.4	0.3	0.05	1.9
Black Space Shuttle Tile	2.3	0.5	0.06	2.7
White Space Shuttle Tile	2.3	0.5	0.06	3.5
Microscope Cover Glass	3.8	0.5	0.05	5.0
ST11 G041-01	2.3	0.3	0.08	3.2

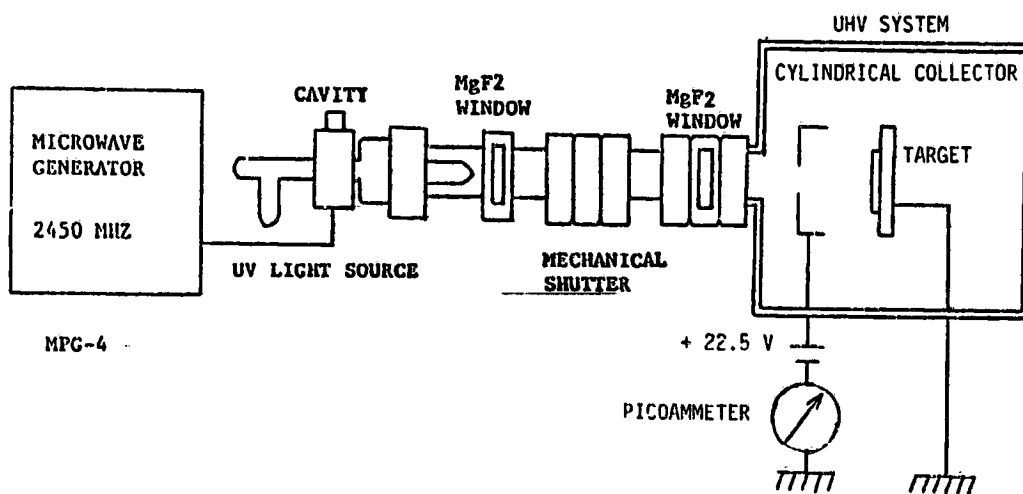


Fig. 1. Schematic diagram of the arrangement for measuring photoyields.

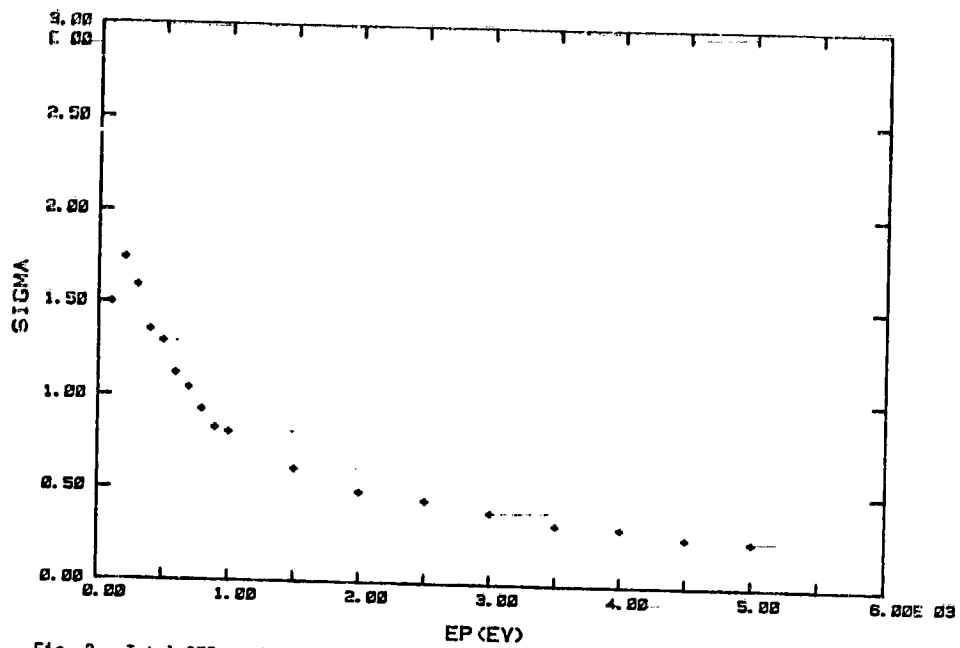


Fig. 2. Total SEE coefficient for Kapton, as-received surface. Single pulse method was used with  $I_p = 60$  nA.

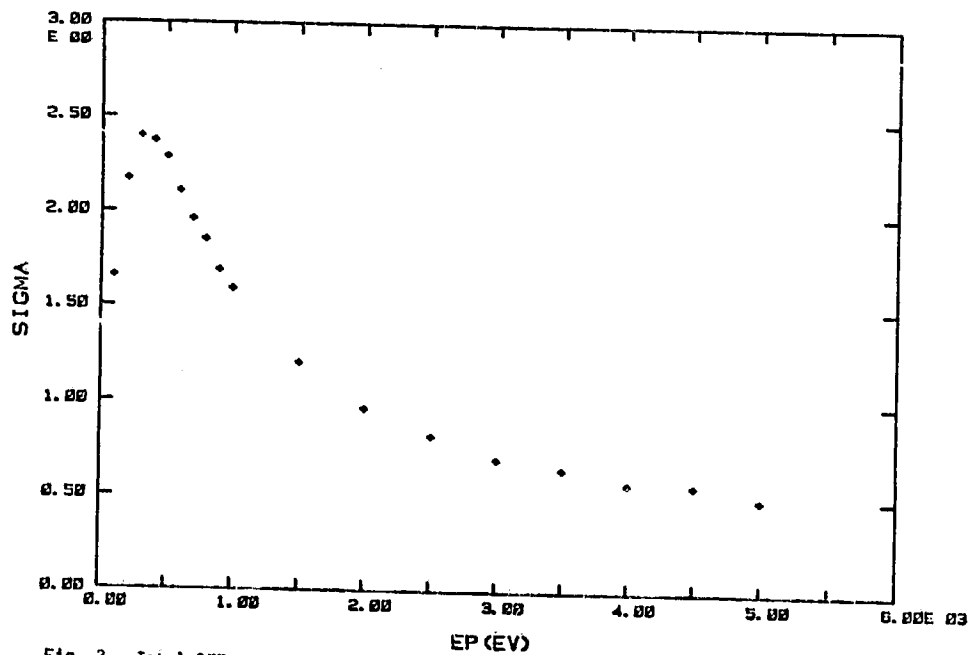


Fig. 3. Total SEE coefficient for FEP Teflon, as-received surface. The single pulse method was used with  $I_p = 60$  nA.

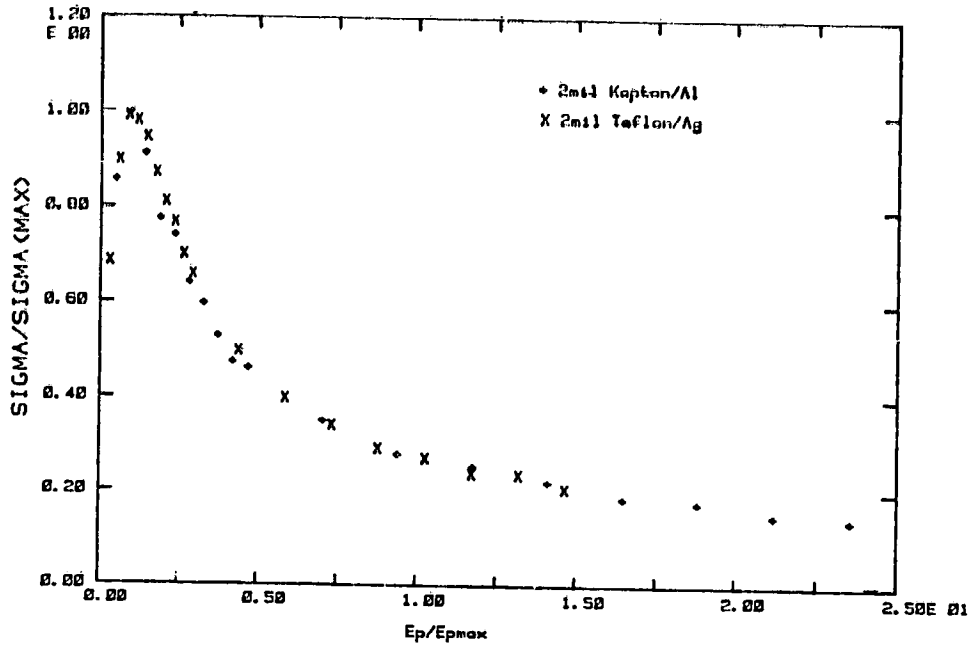


Fig. 4. Normalized total SEE coefficient for Kapton and FEP Teflon compared. Samples and conditions identical to Figs. 2 and 3.

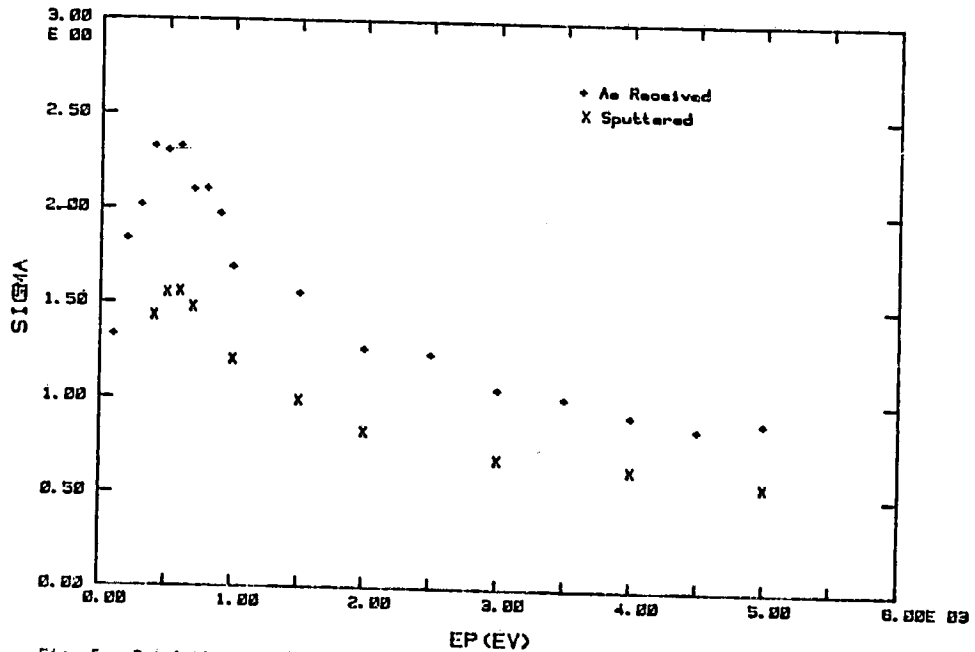


Fig. 5. Total SET coefficient for the white borosilicate shuttle tile surface. Single pulse method was used with  $I_p = 60$  nA.

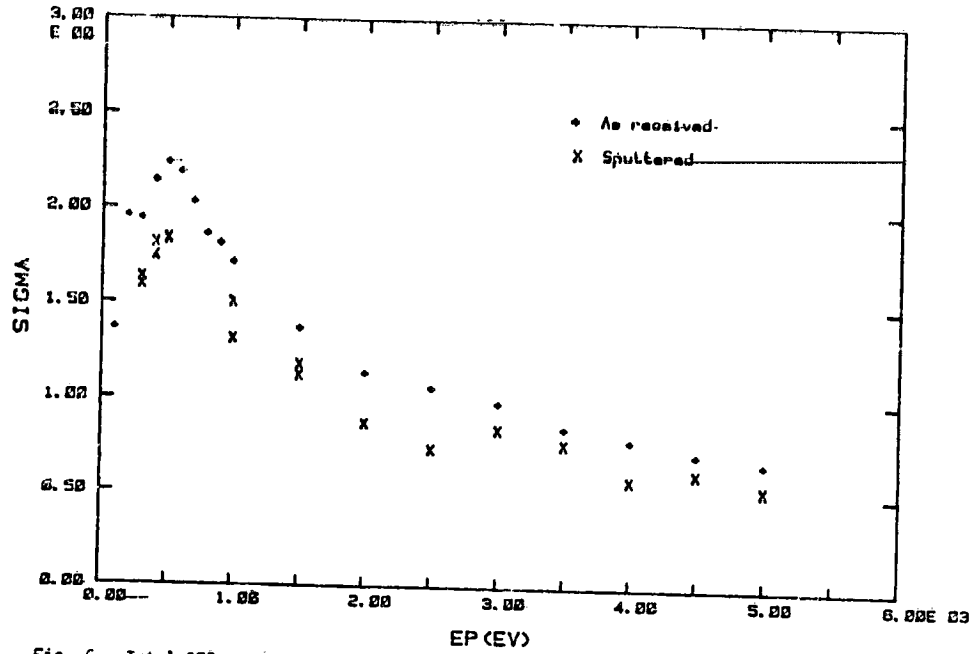


Fig. 6. Total SEE coefficient for black borosilicate surface of the shuttle tile. The single pulse method was used with  $I_p = 60-70$  nA.

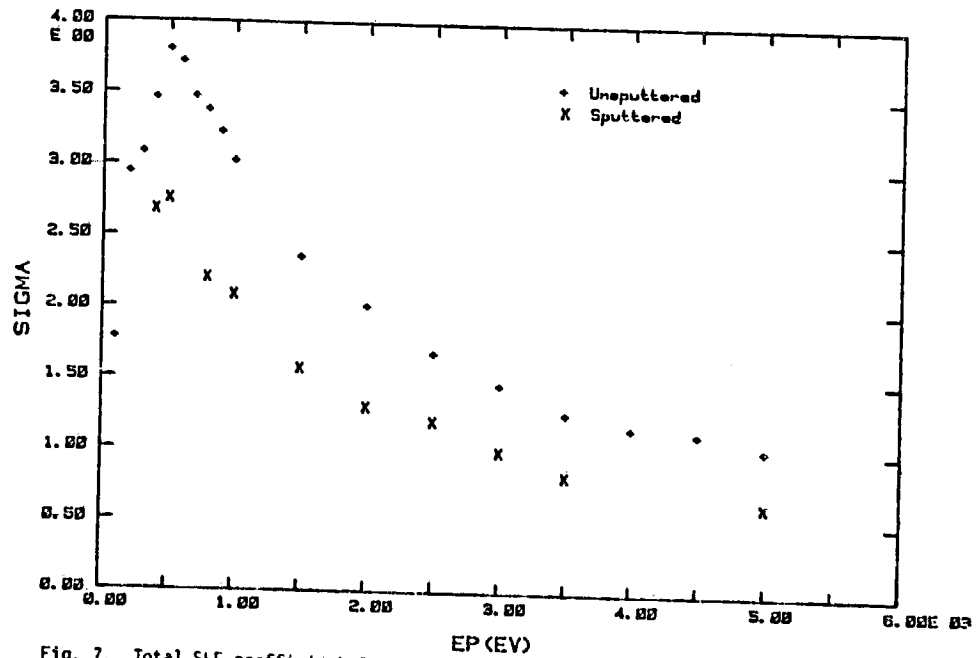


Fig. 7. Total SEE coefficient for microscope slide cover glass, as-received surface. The single pulse method was used with  $I_p = 70$  nA.



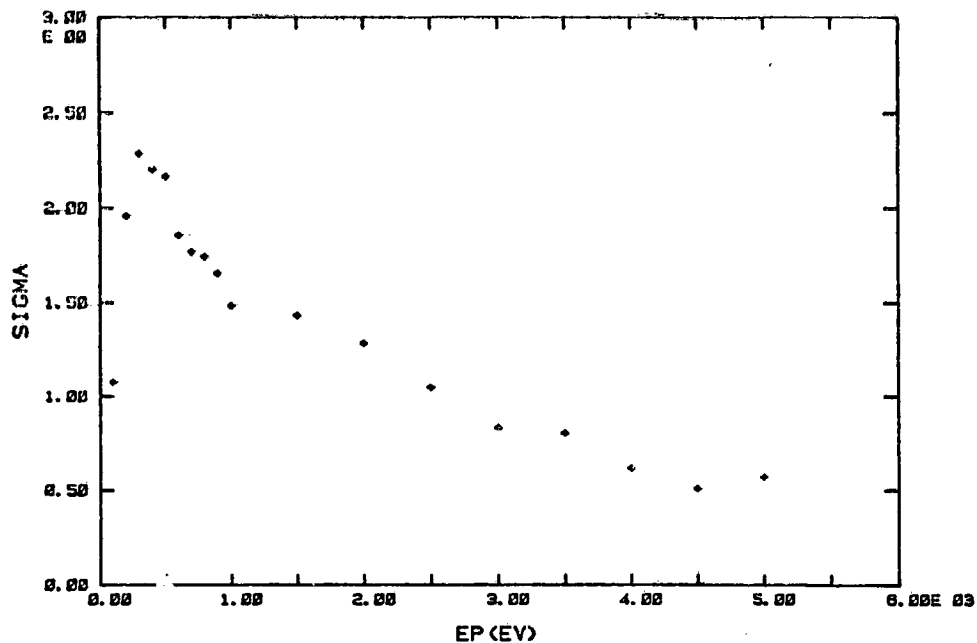


Fig. 8. Total SEE coefficient for the outer fabric of spacesuit material, as-received surface. The single pulse method was used with  $I_p = 60$  nA.

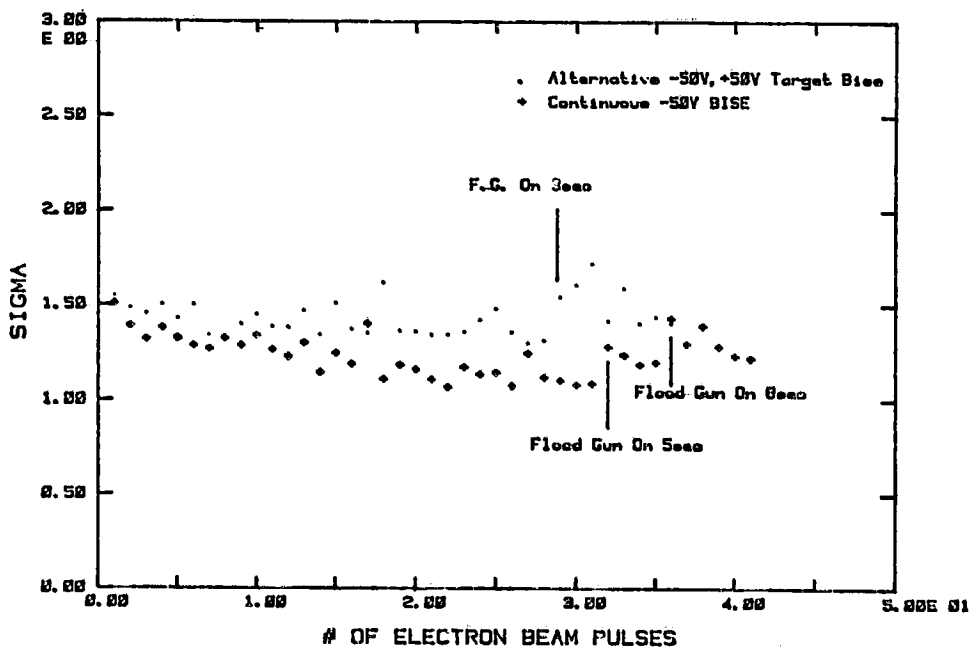


Fig. 9. Changes in total SEE coefficient of the sputtered surface of the white borosilicate glass shuttle tile coating with repeated pulsing to illustrate charging effects in two operating modes. The single pulse method was used with  $I_p = 40$  nA with EP = 500 eV.